J. Membrane Biol. 93, 11–21 (1986)

The Journal of
Membrane Biology

Quantitative Gap Junction Alterations in Mammalian Heart Cells Quickly Frozen or Chemically Fixed after Electrical Uncoupling

J. Délèze and J.C. Hervé
Physiologie Cellulaire, Unité Associée au CNRS no. 290, Université de Poitiers, 86022 Poitiers, France

Summary. The gap junction morphology was quantified in freeze-fracture replicas prepared from rat auricles that had been either quickly frozen at 6 K or chemically fixed by glutaraldehyde, in a state of normal cell-to-cell conduction or in a state of electrical uncoupling. The general appearance of the gap junctions was similar after both preparative procedures. A quantitative analysis of three gap junctional dimensions provided the following measurements in the quickly frozen conducting auricles (mean ± SD): (a) P-face particles' diameter 8.27 ± 0.74 nm (n = 5709), (b) P-face particles' center-to-center distance 10.78 ± 2.12 nm (n = 4800), and (c) E-face pits' distance 9.99 ± 2.19 nm (n = 1600). Corresponding values obtained from chemically fixed tissues were decreased by about 3% for the particle's diameter and about 5% for the particles' and pits' distances. Electrical uncoupling by the action of either 1 mM 2-4-dinitrophenol (DNP), or 3.5 mM n-Heptan-1-ol (heptanol), induced a decrease of the particle's diameter, which amounted to −0.69 ± 0.01 nm (mean ± SE) in the quickly frozen preparations and −0.71 ± 0.01 nm in the chemically fixed ones. The particles' distance was decreased by −0.96 ± 0.04 nm in the quickly frozen samples and by −0.90 ± 0.03 nm in the chemically fixed ones and the E-face pits' distance was similarly reduced. All differences were statistically significant ($P < 0.001$ for all dimensions). Electrical recoupling after the heptanol effect promoted a return of these gap junctional dimensions towards normal values, which was about 50% complete within 20 min. It is concluded that very similar morphological alterations of the gap junctional structure are induced in the mammalian heart by different treatments promoting electrical uncoupling and that these conformational changes appear independently of the preparative procedure. The suggestion that the observed decrease of the particles' diameter is genuinely related to the closing mechanism of the unit cell-to-cell channel set in their centers is thus confirmed.

Key Words mammalian heart · cell-to-cell conduction · cell-to-cell conduction block · electrical uncoupling · gap junction · quantitative gap junction electron microscopy · quick-freezing at 6 K

Introduction

The communicating junctions of electrically connected cells can be switched to a nonconducting state (for a review, *see* Loewenstein, 1981). Decreases in the size and distance of the gap junctional particles correlating with this electrical uncoupling were first described at the crayfish electrical synapses (Peracchia & Dulhunty, 1976) and analogous structural transitions have also been reported in the gap junctions of mammalian liver and gastric epithelium (Peracchia, 1977) and of heart Purkinje fibers (Délèze & Hervé, 1983). Since the junctional particles (the connexons) build up the only structural elements bridging the gap between the membranes of adjacent cells, it is natural to suggest that their shrinkage on electrical uncoupling reflects a conformational change related to the regulation of the cell-to-cell channel permeability. However, two reasons for caution with this interpretation should be mentioned. First, in two studies of heart Purkinje fibers, the particle diameter was reported to increase after uncoupling treatments (Dahl & Isenberg, 1980; Shibata & Page, 1981), although particle distance was decreased as in the original observations of Peracchia and Dulhunty (1976) and of Peracchia (1977). Secondly, it is questionable that communicating cell junctions can be fixed in the conducting state, since the cell-to-cell conductance decreases quickly during glutaraldehyde fixation, both in the crayfish electrical synapse (Politoff & Pappas, 1972) and in heart Purkinje fibers (Délèze & Hervé, 1983). These uncertainties prompted us to analyze the structure of the conducting gap junctions and its modifications after electrical uncoupling in quickly frozen mammalian heart preparations and to compare the results to those obtained from chemically fixed tissues. This research has been reported in a preliminary form (Délèze & Hervé, 1984).

Materials and Methods

Preparations

We had to find a suitable heart preparation, as with the cold metal block quick-freezing technique we intended to apply, the thickness of tissue that can be preserved in a satisfactory state

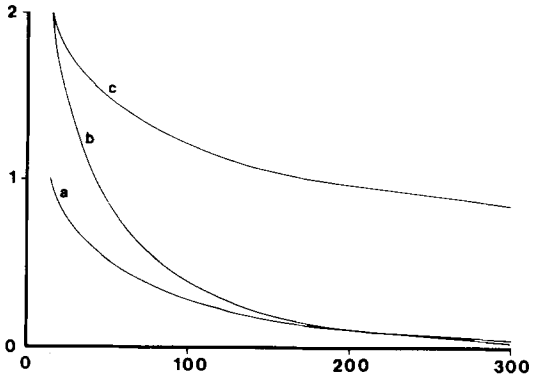

Fig. 1. Effects of changing independently two parameters of the Bessel function (Eq. 1) describing the spread of electrotonic potentials in the rat auricle. *Abscissa:* distance (x) from the current source (μm). *Ordinate:* steady-state displacement of membrane potential (V) during constant current pulses (relative units). Curve (*a*): control conditions ($\lambda_{(a)} = 150$ μm). Curve (*b*): after a rise of R_i to such a size (2.32×) that V is doubled at $x = 15$ μm ($\lambda_{(b)} = 98.5$ μm). Curve (*c*): after the same rise of V at $x = 15$ μm caused by an increase of R_m (164.5x; $\lambda_{(c)} = 1924$ μm). Note that V at short distances is nearly insensitive to changes in R_m but is a good indicator of R_i, and that although a change of R_i or of R_m can have the same effect on V at short distances, they are easily distinguished by the potential values at larger distances

for a detailed morphological study without cryoprotectants is limited to a layer about 12 to 15 μm thick (Escaig, 1982) by the rapid growth of ice crystals at greater distances from the cold surface where the cooling rate becomes too slow. It was found that the first layer of cardiac cells underneath the thin endocardium of right auricles from rat hearts could often be frozen, with the apparatus mentioned below, in a state of preservation allowing a good resolution of the gap junctional structure, which was not regularly accomplished with other parts of the same heart such as the papillary muscles. All measurements were therefore performed on rat auricles. The animals (mongrels or Long Evans) were stunned by a blow on the head, the hearts rapidly removed, the auricles dissected and cut into approximately flat sheets, measuring from about 25 to 50 mm^2, which were kept at room temperature in an oxygenated Tyrode solution containing (in mM): 5 glucose, 137 NaCl, 1.8 $CaCl_2$, 1 $MgCl_2$, 12 $NaHCO_3$, 0.4 NaH_2PO_4 and 5.4 KCl. The solutions were saturated with a 5% CO_2 in O_2 mixture giving a pH of 7.2. All experiments were performed at 22°C.

Uncoupling Procedures

Cell-to-cell conduction block was induced either by the uncoupler of oxidative phosphorylation *2-4-dinitrophenol* (DNP) at a 1 mM concentration in Tyrode solution, or by the *heptyl alcohol n*-Heptan-1-ol (heptanol), 3.5 mM in Tyrode. DNP has been shown to depress junctional conductance in the salivary gland cells of *Chironomus* (Politoff et al., 1969) and has a similar action on the electrical transmission in heart Purkinje fibers (De Mello, 1979; Dahl & Isenberg, 1980; Délèze & Hervé, 1983). The blocking action of heptanol on the electrical synapse of the crayfish giant axon was discovered by Johnston et al. (1980), and a similar action on cell-to-cell conduction has been observed in the rat gastric epithelium, the rat pancreas, the *Xenopus* embryo (Bernardini et al., 1982, 1984) and in heart Purkinje fibers (Délèze & Hervé, 1983). The effects of heptanol are completely reversible within 10 to 20 min of washing the substance, which is not the case with DNP treatment. This reversibility of the uncoupling by heptanol prompted us also to examine the gap junction morphology after electrical recoupling.

States of Electrical Coupling

In the auricle, single rows of electrically coupled cells, of diameter $d = 15$ μm and of length $h = 100$ μm, build up fibers with cable properties which are furthermore arranged into a grid network by numerous lateral connections. Woodbury and Crill (1961) have investigated the conduction of a subthreshold change of membrane voltage induced by applying current pulses at an intracellular point. They showed that the passive electrical properties of this structure are analogous to those of a thin unbounded planar cell, in which the steady-state spatial decrement of voltage is described by a Bessel function. A more complete theoretical treatment can be found in Noble (1962), and the analogous cases of the ventricular walls of the mice heart (Tanaka & Sasaki, 1966) and of monolayer cultures of rat heart cells (Jongsma & van Rjin, 1972) have also been experimentally and mathematically considered.

In a conducting auricle, the decrement of the steady-state voltage V at the distance x from the point of application of a current of intensity I_o fits the equation

$$V_x = I_o R_i / 2\pi d K_{o(x/\lambda)} \quad (1)$$

where R_i is the resistivity of the intracellular material including the contribution of the cell junctions to the total internal resistance, K_o is a modified Bessel function of the second kind (Abramowitz & Stegun, 1964) and $\lambda = (R_m d/2R_i)^{1/2}$ is the length constant, with R_m the resistance of one unit area of the surface membrane in Ω cm^2.

Woodbury and Crill (1961) also pointed out that current spread in the auricle varies with direction, the space constant they measured parallel to the great axis of the fiber (130 μm) being twice that perpendicular to the fiber direction, with isopotential contours approximating ellipses. All measurements in our experiments were therefore taken in the fiber direction only. The position of the intracellular microelectrodes used for current injection and voltage measurements was controlled at a magnification of 400×, using Nomarski's optics which provide a satisfactory image of the fiber surface and outline but do not allow to recognize the position of the intercalated disks. Average values of V_x obtained on several auricles are indicated in Fig. 4 (circles) together with a theoretical curve constructed from Eq. (1) and fitted to the points by a trial-and-error least-squares test which yielded a value of 150 μm for λ. Woodbury and Crill (1961) already concluded from this type of voltage spread that the cells are electrically coupled.

Instead of the laborious procedure illustrated by Fig. 4 (circles), the presence of a propagated action potential, either spontaneous in a majority of cases or in answer to electrical stimulation in a few others, was employed as an obvious simple test of normal cell-to-cell electrical coupling. The propagated mechanical activity that follows the action potential was also routinely observed up to the instant of fast freezing as a convenient control of maintained electrical coupling.

The action of the uncoupling agents was estimated by observing the characteristic changes that occurred in the shape of

the spatial voltage decrement when the cell-to-cell conductance was progressively decreased and finally became blocked. It is obvious from the topography of the auricle that the junctional resistances r_j are in series with $r_i = 4R_i h/\pi d^2$, the internal resistance of the unit length of component cable. Discontinuities in the cytosolic conductor caused by the cell-to-cell resistance do not, however, manifest as a stepwise decrement of membrane voltage with distance in the normal conducting state because the voltage steps in these conditions are smaller than the standard error of the mean voltage measurements and the spatial potential spread is therefore experimentally identical with that given by Eq. (1). This situation is often referred to as r_j being lumped with r_i. If after a moderate rise r_j still appears lumped with r_i, it is readily seen from Eq. (1) that V_x becomes larger at small values of x, and falls off more steeply with distance since λ decreases as $R_i^{1/2}$. Figure 1 (curve *b*) illustrates the theoretical effect of a 2.32× increase of R_i, which raises V at $x = 15$ μm by a factor 2, on the potential distribution. The same rise of V at $x = 15$ μm could also be caused by a large increase of R_m (164.5×), but then the fall of potential with distance would look quite different since λ would rise to about 13× its initial value (Fig. 1, curve *c*).

When electrical uncoupling proceeds, r_j becomes more important relative to r_i and the main internal resistance will actually be located at the cell-to-cell membranes, making voltage steps appear at the cell boundaries (*see* Socolar & Loewenstein, 1979, Appendix A, for the mathematical solution of an analogous case). An example of a spatially discontinuous potential distribution obtained on auricle cells treated by DNP is shown in Fig. 2*a*.

If uncoupling proceeds to a degree where very little or no current flows through the junctions, the cytoplasms of the individual cells become isolated from each other and the unbounded whole is broken down to its component units. The voltage across the reduced membrane area of one single cell now available for current flow, measurable at short distances from the current source, will be larger than in the controls and it will fall off abruptly across the nearest cell boundaries, as shown in the typical example of Fig. 2*b*. Since the intercalated disks, which contain the gap junctions, cannot be observed on the living heart fibers, the cut-off of the voltage deflection at a distance $x < h$ is ascertained by the procedure illustrated in Fig. 4, squares and interrupted curve.

The action of the uncoupling agents was essayed until it was established that 1 mM DNP or 3.5 mM heptanol would regularly promote uncoupling. When the action of either substance was fully developed after 10 to 15 min, the cells were as a rule isolated as in Fig. 2*b*. No attempt to distinguish this case from the less frequent type of uncoupling illustrated by Fig. 2*a* was made in the morphological study.

Conventional 2 M KCl-filled microelectrodes of 20 to 30 MΩ resistance were employed with high-impedance, capacity-compensated input stages, one of them (M-707, W.P.I., New Haven, Conn.) having current-passing capability. The bridge balance circuitry, which should in principle allow for current passing and voltage recording through the same microelectrode, was, however, not employed to avoid uncontrollable errors caused by large random fluctuations of the microelectrode resistance. Instead, the voltage deflection was always measured with a separate electrode even at short distances.

Fixation by Fast-Freezing

Four sets of auricles were fixed by fast-freezing: (1) auricles with normal conduction, (2) auricles treated by DNP for 15 to 20 min, (3) auricles treated by heptanol for 15 to 20 min, and (4) auricles recoupled after the heptanol effect. Ultrarapid cryofixation was performed by projection of tissue samples onto the polished surface of a cold metal block (van Harreveld & Crowell, 1964; Heuser et al., 1976; Schwabe & Terracio, 1980) by means of an apparatus (Cryoblock, Reichert-Jung, Paris) designed by Escaig (1982). A copper block maintained under a vacuum is cooled to approximately 6 K by an internal circulation of liquid helium. When the low temperature is attained, gaseous helium is admitted into the vacuum chamber until the reaching of atmospheric pressure releases a spring that opens a shutter and triggers tissue projection onto the block. This procedure prevents icing and contamination of the copper surface by contact with the atmosphere prior to tissue freezing. The frozen specimens are then stored in liquid nitrogen until freeze-fracturing can be performed.

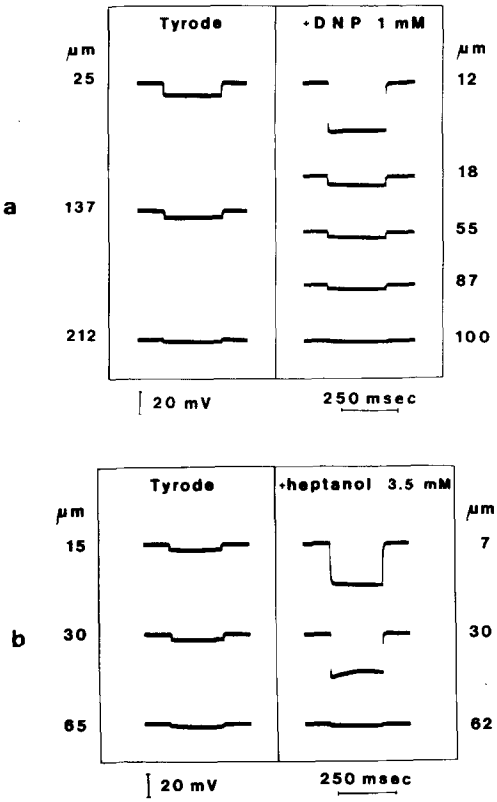

Fig. 2. Membrane potential records obtained at several distances from an intracellular point where current is applied. Rat auricles in control conditions (Tyrode) and 15 min after addition of an uncoupler of cell-to-cell communication: (*a*) DNP, (*b*) heptanol. The intensity of current pulses was 2.5×10^{-8} A in (*a*) and 1×10^{-8} A in (*b*)

Chemical Fixation

Three other series of preparations: (1) auricles with normal conduction, (2) auricles treated by DNP for 15 to 20 min, and (3) auricles recoupled after the heptanol effect, were chemically fixed by 1.25% glutaraldehyde in Tyrode's solution (pH 7.2) at 22°C for 2 hr and cryo-protected before freeze-fracturing by successive immersions in solutions of rising glycerol concentrations (10, 20 and 30% in water). The same procedure had been previously followed in the preparation of sheep Purkinje fibers (Délèze & Hervé, 1983).

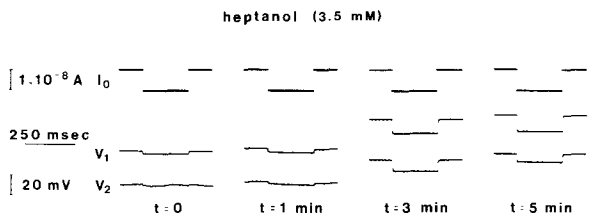

Fig. 3. Early heptanol effects on a rat auricle. *From top to bottom:* calibration of current pulses, membrane voltage deflection at 20 and at 125 μm from the point of current application. The heptanol containing Tyrode's solution is admitted at time $t = 0$

Freeze-Fracturing

The quickly frozen specimens were transferred from the liquid N_2 to the cold freeze-fracture chamber under a cover of frozen freon 22 to prevent rewarming and icing. Freeze-fracturing was carried out at -120°C under a vacuum of at least 10^{-6} Torr in a Balzers BAF 300 apparatus. Preparation of the replicas followed the same standardized procedure mentioned previously (Délèze & Hervé, 1983). To minimize the possible effect of differences in the amount of shadowing material on the particle size, three specimens from preparations chemically fixed in different functional states were platinized simultaneously. This procedure could not, however, be used with the much larger freeze-fracture faces obtained from the quickly frozen tissues. Instead, several samples that had been frozen in different functional states were platinized in a random order in the same run. With these precautions, slight variations in the amount of shadowing material should not become systematically related to the functional state of the preparation.

Electron Microscopy and Image Analysis

122 fracture faces obtained from 61 auricles were examined under a Jeol 100C electron microscope and yielded 460 micrographs of gap junctions. The electron microscope magnification was checked with a carbon grid (no. 1002, E.F. Fullam) in every run of observations. All micrographs were oriented to get the direction of platinum shadowing from bottom to top. The designation of fracture faces is conventional.

Three morphological dimensions of the gap junctions were measured manually on positive prints at an enlargement of 300,000×: (I) P-face particle diameters by means of a TGZ 3 (Carl Zeiss) particle size analyzer, which allows for optical superposition of the particles' images with a light beam. The diaphragm setting at coincidence provides an accurate measurement; (II) P-face particles' center-to-center distances and (III) E-face pits' distances measured by means of an IBAS I (Kontron) image analysis system. The dimension at the base of the particles perpendicularly to the shadowing direction was taken as the particle diameter. According to the generally accepted interpretation of the freeze-fracture replicas of gap junctions (McNutt & Weinstein, 1970), the particle level where this measurement is taken should correspond to approximately mid-distance from the hemi-connexon ends. Only well-delineated particles were selected for measurement and those showing common edges or optically superimposed bases were rejected. As discussed previously (Délèze & Hervé, 1983), these strict criteria minimize the errors due to the impossibility of recognizing the limits of confluent particles and also reduce the effect of variations in the platinum thickness dependent on particle tightness, since most measurements are thus performed outside the densely packed areas.

Junctional areas large enough to provide about 400 particle diameter measurements according to the above-mentioned criteria were selected for quantitative analysis. The center-to-center distances were measured between particles chosen at random on the same junctions and all their nearest neighbors, including the tightly packed and confluent ones.

Results

Effects of DNP on the Cell-to-Cell Junctional Communication

The first effect of 1 mM DNP is a decrease of the length constant (λ) caused by a rise of the intracellular resistivity (R_i), detected by the electrotonic voltage becoming larger at short distances from the point of current application and falling off more rapidly with distance (*see* Fig. 1, curves *a* and *b*). Discontinuities in the spatial decrement of voltage at intervals corresponding to one cell length, such as those shown in Fig. 2*a*, become detectable after about 7 min. This appearance of voltage steps in a network with cable properties reflects the division of the previously continuous intracellular conductor into segments by the development of high transverse resistances, located at the intercalated disks, when a substantial number of connecting elements in the communicating cell junctions have been switched to the nonconducting state. Confirmation of this interpretation is provided by the correspondence between the spacing of the voltage discontinuities and the value of the cell length. In the instance of Fig. 2*a*, two voltage steps at 12 μm $< x <$ 18 μm and at 87 μm $< x <$ 100 μm are separated by a much less steep incline between 18 and 87 μm. The expanded cell model of Woodbury and Crill (1961) with continuous voltage distribution has obviously become inadequate and a two-dimensional network of short cables connected by resistances, similar to that considered by Brink and Barr (1977) for the earthworm giant axon, would provide a more appropriate description of the passive electrical properties. The voltage decrement in a short cable is less steep than in the unbounded cable (Weidmann, 1952), and *a fortiori* even less so than in the unbounded planar cell, which accounts for the nearly even potential level observed between two abrupt steps (Fig. 2*a*).

Uncoupling by DNP usually proceeds further until, at times larger than 10 to 15 min, the induced membrane voltage is mainly confined to the cell wherein current is applied, as shown by the series of measurements reported in Fig. 4*a* (squares and

interrupted line). In this case the average voltage change at short distances is about twice that recorded with the same current when the cells were electrically coupled (circles and continuous line). This rather moderate rise indicates that DNP has the additional effect of decreasing the resistance of the nonjunctional membrane. The spatial voltage decrement is abruptly interrupted at a farther distance which in all trials was found to be shorter than cell length. The meaning of this observation becomes clear if it is recalled that the relative positions of the microelectrode and of the nearest cell boundary cannot be stated on the living preparation and therefore the electrotonic voltage will be seen to vanish at the average distance $x = h/2$ when the junctional resistance becomes very high. Once established, uncoupling by DNP is not reversible by washing the auricles with Tyrode's solution.

Effects of Heptanol on the Cell-to-Cell Junctional Communication

Shortly after the addition of heptanol, the membrane voltage induced by intracellular pulses of constant current (Fig. 3, records at 1 and 3 min) is more increased, relative to its control value, at the longer distance (V_2 at 125 μm) than at the shorter one (V_1 at 20 μm) from the point of current injection. According to the graphical analysis (Fig. 1) of the effects of varying R_i or R_m in Eq. (1), these early changes indicate an increase of λ caused by a rather large rise of R_m, possibly but not certainly associated with a rise of R_i. Later on, however, (Fig. 3 at 5 min) V_1 increases further while V_2 is getting smaller. This particular association of membrane potentials varying in opposite directions can only be accounted for by a decrease of λ caused by a rise of R_i. It is readily seen from Eq. (1) and Fig. 1 that a decrease of λ due to R_m becoming smaller would tend to reduce V at the shorter distance also.

A steady-state effect of heptanol illustrated by the sample records of Fig. 2*b* is reached within 10 to 15 min. By then the induced voltage is further increased and nearly uniform at short distances, in this example between 7 and 30 μm, and it falls down to a very low value between 30 and 62 μm. This discontinuous voltage distribution conforms to that expected for a cardiac cell that has become virtually disconnected from its neighbors.

The average membrane potentials obtained at different distances during the steady-state action of heptanol on several preparations are indicated in Fig. 4*b* (squares and interrupted line), for comparison with the spatial decrement of voltage in auricles with normal cell-to-cell conduction (circles and continuous line). That all attempts failed to detect a

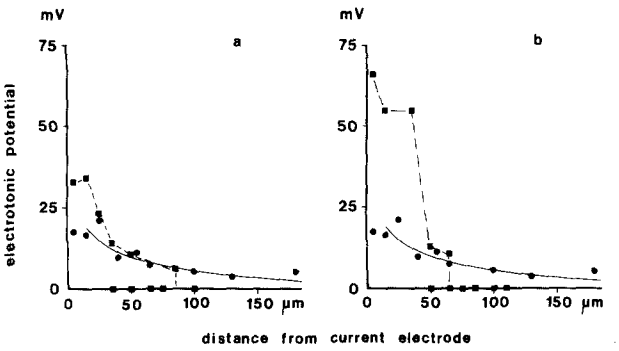

Fig. 4. Spatial decrement of membrane potential along the fiber's great axis in rat auricles with normal cell-to-cell conduction (●) and after electrical uncoupling (■) by: (*a*) 1 mM DNP, (*b*) 3.5 mM heptanol. Each point indicates the mean of several measurements obtained on 11 auricles made quiescent by 5×10^{-4} M carbamyl-β-methylcholine. Current pulses of constant intensity (I_O) were employed throughout the same experiment, but I_O varied between 1 and 5×10^{-8} A in different preparations. For comparison of the data, the voltages reported on the abscissa have been multiplied by 5×10^{-8} A/I_O. The continuous line in (*a*) and (*b*) indicates the Bessel function (Eq. 1) fitted to the control voltage measurements (●) by a trial-and-error least-squares test which provided a value of 150 μm for λ. The interrupted lines drawn across the average measurements (■) obtained during the steady-state effects of either substance indicate a sharp cut-off of the voltage deflection at a distance shorter than one cell length. The distance at which the induced membrane potential fell to zero was randomly distributed since the cell boundaries could not be recognized during the experiment

voltage deflection beyond a distance of about 65 μm, somewhat shorter than the average cell length, despite the large membrane potential change measured close to the current electrode, is considered a significant test of electrical uncoupling.

The resting potential was usually very low during heptanol action. When auricles that had been depolarized and electrically uncoupled by heptanol were returned to the Tyrode's solution, resting membrane potential, excitability and spontaneous activity with propagated action potentials were restored within 10 min, together with a normal cell-to-cell electrical coupling.

Morphological Correlates of Electrical Uncoupling Measured on Gap Junctions from Quickly Frozen Auricles

Gap junctions are less frequently found in the relatively small cells of the rat auricle than in the larger ones of the sheep Purkinje fibers. Typical examples of fracture faces from auricles quickly frozen in the conducting state are shown in Figs. 5 and 6*a*. The gap junctions present their characteristic aspect of P-faces with irregular aggregates of attached parti-

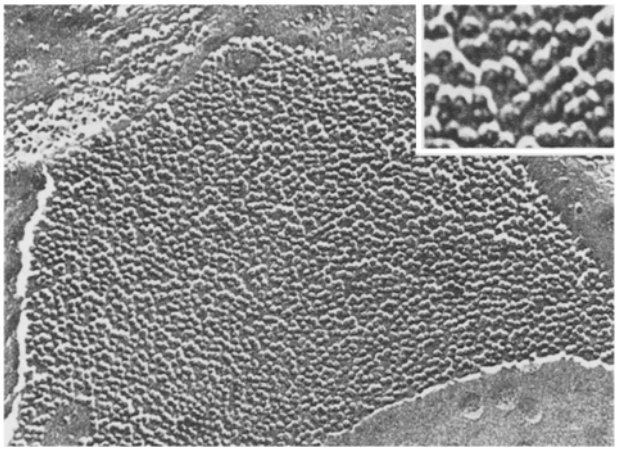

Fig. 5. P-face freeze-fracture replica of a gap junction from a rat auricle quickly frozen in a state of normal cell-to-cell electrical conduction. Magnification 100,000×. *Inset:* enlarged part (300,000×) of the same junction showing a central depression, which might correspond to the opening of an axial hydrophilic channel, on top of most particles

cles, and occasional E-faces punctuated with small pits. In some areas a central crater can be seen on the top of most particles (Fig. 5, inset).

A quantitative analysis of gap junction images from auricles quickly frozen in the conducting state (Figs. 5 & 6*a*), or in a state of cell-to-cell conduction block induced by the action of either heptanol (Fig. 6*c*) or DNP, shows a statistically significant reduction of the average values of the P-face particles' diameter and center-to-center spacing and of the E-face pits' distance (Fig. 7*a* and Table). The distribution of the particles' diameters (left histogram in Fig. 7*a*) is nearly symmetrical around a mean (± SD) of 8.27 ± 0.74 nm in the conducting state, which decreases to 7.58 ± 0.65 nm after conduction block. The distribution of the particles' distances shows some asymmetry with a positive skewness (middle histogram in Fig. 7*a*) which becomes more pronounced when the mean distance decreases, from 10.78 ± 2.12 nm in the coupled cells to 9.82 ± 1.70 nm after electrical uncoupling. The translation of the distribution towards smaller distances seems to be restricted at about 5 nm, as shown by the stable values of the frequencies in the two smaller classes. This limitation indicates that the particles cannot get closer to each other than this distance minimum and also provides a simple explanation for the asymmetry of the distribution: clearly, there is more constraint on the shorter distances than on the larger ones. Similar comments can be made on the E-face pits' distances (right histogram in Fig. 7*a*).

The measured gap junctional dimensions appear somewhat more reduced after uncoupling by DNP than after heptanol action (Table), which might be related to the irreversible character of DNP, but not of heptanol, uncoupling.

Morphological Correlates of Electrical Uncoupling Measured on Gap Junctions from Chemically Fixed Auricles

The results of the quantitative image analysis performed on auricles that had been glutaraldehyde fixed in the conducting state (Fig. 6*b*), or after uncoupling by either DNP (Fig. 6*d*) or heptanol, are presented in Fig. 7*b* and in the Table. The general result is qualitatively very similar to that obtained on quickly frozen preparations and can be described as a statistically significant decrease of all the measured dimensions (Table). The positive asymmetry of the frequency distributions of the particles' and pits' distances (Fig. 7*b*) also tends to be slightly accentuated as in the quickly frozen preparations.

Effects of Electrical Recoupling on Gap Junctional Dimensions

A quantitative analysis was performed on gap junction pictures obtained from quickly frozen (Fig. 6*e*) or chemically fixed (Fig. 6*f*) auricles that had been first submitted to the uncoupling action of heptanol for 20 min and then washed free of heptanol with Tyrode solution for 20 to 120 min before freezing or chemical fixation. Recovery of electrical coupling as shown by a propagated electrical and mechanical activity took place within 10 to 15 min. The values assumed by the three gap junctional dimensions in the electrically recoupled cells are reported in the Table. All the means increase again towards those observed in control conditions and about half of the dimensional changes caused by uncoupling are reversed within a relatively short time (from about 20 to 120 min) after electrical recoupling. No morphological difference could be detected between the gap junctions of auricles that had been quickly frozen or chemically fixed earlier (within 30 min) or later (from 1 to 2 hr) after electrical recoupling.

Quantitative Comparison of Gap Junctions Quickly Frozen or Chemically Fixed in Three Functional States

In every functional state of the cell-to-cell electrical communication (cells coupled, uncoupled or recoupled), the mean gap junctional P-face particles' diameter and distance and the mean pits' distance are slightly smaller (3 to 5%) in the chemically fixed

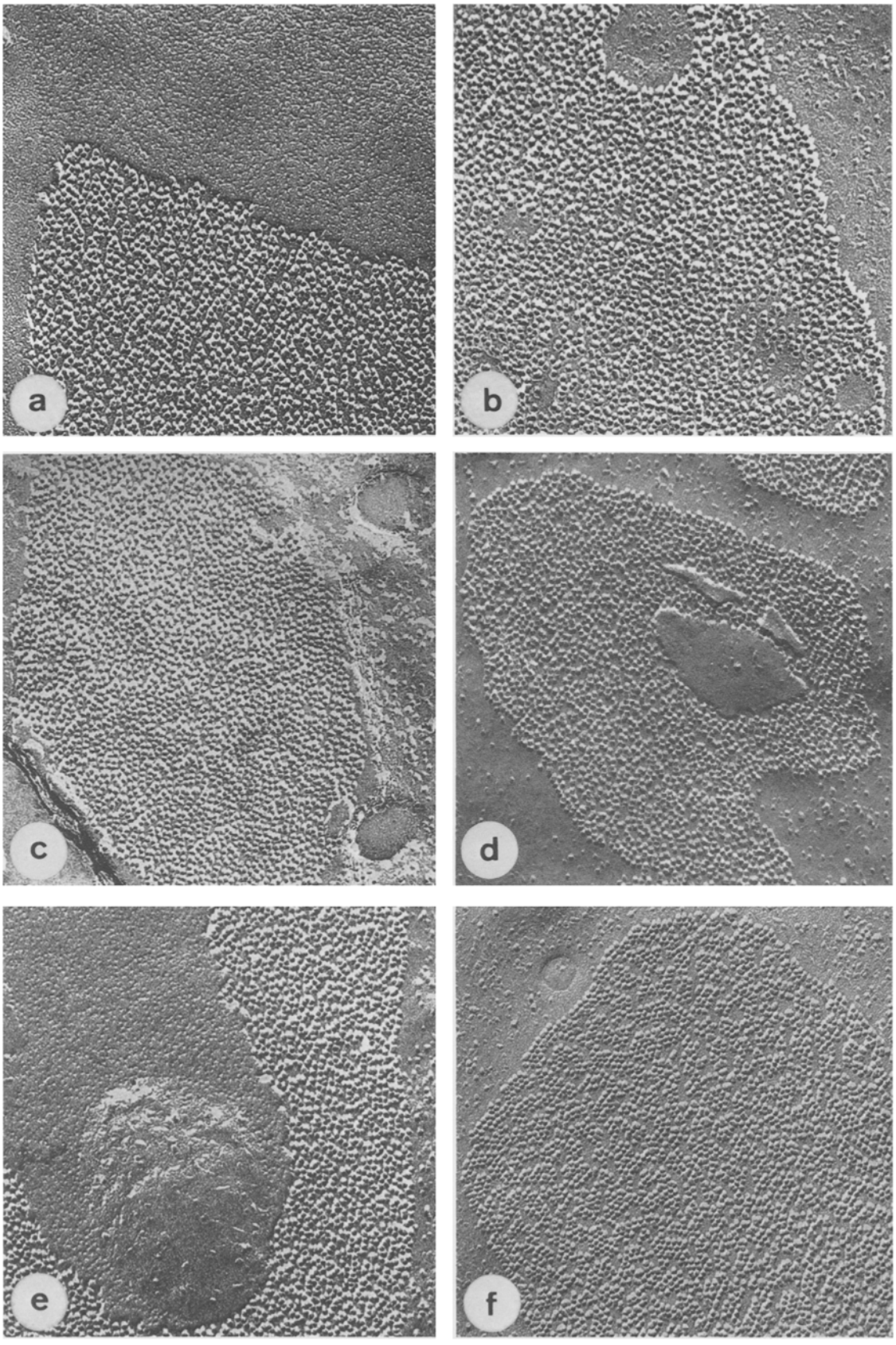

Fig. 6. Sample freeze-fracture replicas of gap junctions from quickly frozen (left pictures) or glutaraldehyde-fixed (right pictures) rat auricles: (*a*,*b*) electrically coupled, (*c*) electrically uncoupled by heptanol, (*d*) electrically uncoupled by DNP, (*e*,*f*) electrically recoupled after the washing of heptanol. Magnification 100,000×

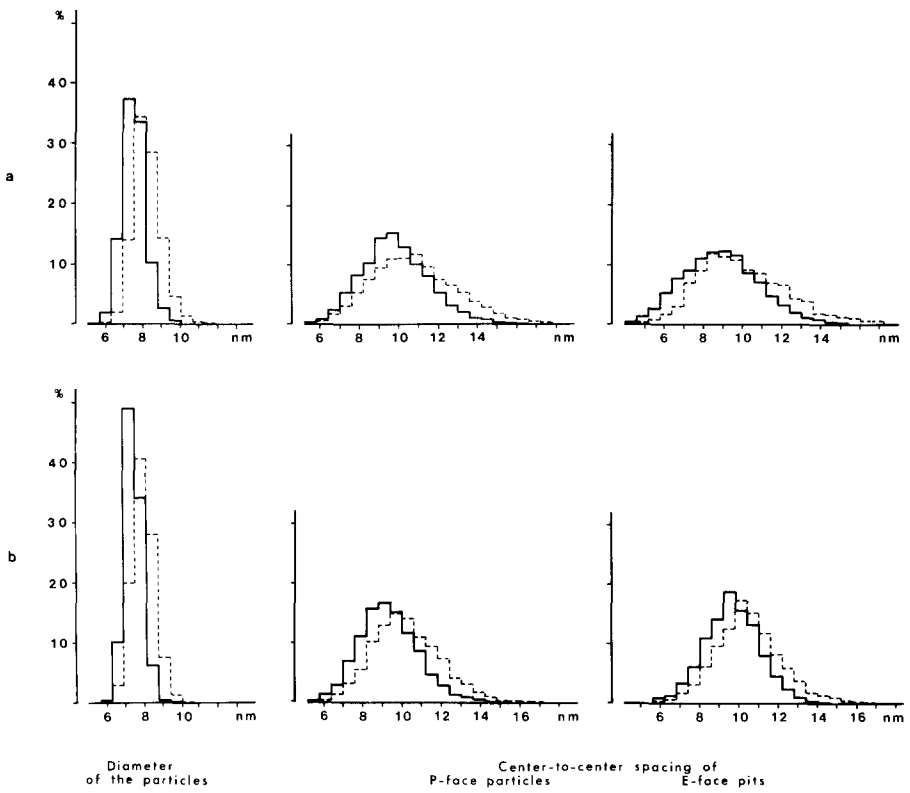

Fig. 7. Size distributions of three gap junctional dimensions in electrically coupled rat auricles (dotted lines) and after electrical uncoupling (continuous lines): (*a*) quickly frozen; (*b*) glutaraldehyde-fixed preparations. *See* Table for the statistical parameters

Table. Dimensions measured in quickly frozen and chemically fixed gap junctions from conducting and nonconducting auricles[a]

State of electrical coupling	Preparative mode	P-face particles' diameters		P-face particles' spacings		E-face pits' spacings	
		n[b]	mean ± SD[c]	n	mean ± SD	n	mean ± SD
coupled	quick-freezing	5709	8.27 ± 0.74	4800	10.78 ± 2.12	1600	9.99 ± 2.19
	chemical fixation	4450	8.09 ± 0.61	4000	10.20 ± 1.70	4800	9.48 ± 1.66
heptanol-uncoupled	quick-freezing	3689	7.71 ± 0.73	3600	9.93 ± 1.70	1600	9.06 ± 1.92
DNP-uncoupled	quick-freezing	5673	7.49 ± 0.57	5600	9.75 ± 1.70	2800	8.78 ± 1.88
pooled data heptanol and DNP-uncoupled	quick-freezing	9362	7.58 ± 0.65	9200	9.82 ± 1.70	4400	8.88 ± 1.90
DNP-uncoupled	chemical fixation	5203	7.38 ± 0.48	5600	9.30 ± 1.47	6000	8.65 ± 1.43
recoupled after heptanol	quick-freezing	6835	8.02 ± 0.60	8400	10.25 ± 1.70	4400	9.44 ± 1.90
recoupled after heptanol	chemical fixation	5600	7.62 ± 0.53	5600	9.73 ± 1.71	4800	8.99 ± 1.47

[a] Comparisons of the means obtained from similarly prepared auricles in different states of electrical coupling show that all differences are statistically significant ($P < 0.001$). The means of the samples quickly frozen or chemically fixed in the same state of electrical coupling also differ significantly ($P < 0.001$).
[b] n Number of measurements.
[c] SD Standard deviation.

than in the quickly frozen auricles (Table). Figure 8 indicates the change in size corresponding to electrical uncoupling and recoupling for each measured dimension in the quickly frozen (interrupted lines) and in the chemically fixed samples. The measurements obtained in the two series differ only by an approximately constant vertical translation, as expected for a small systematic size difference. Furthermore, the variations of the mean measurements observed after uncoupling and recoupling are very similar in both series and therefore they do not appear to depend on the preparative procedure.

It may be finally interesting to note that even in the gap junctions in which the cumulated effects of chemical fixation and of uncoupling reduces the particles' and pits' distances to the minimum ob-

served in our experiments (Fig. 8*b* and *c*, state II, lower curves), the gap junctional particles' arrangement never looks crystallized nor hexagonal, neither do the usually more regularly arranged E-face pits. But in electrically recoupled cells, small hexagonally ordered aggregates of a few densely packed particles separated by smooth membrane alleys are frequently observed (Fig. 6*f*).

Discussion

Quick-Freezing versus Chemical Fixation on Gap Junction Structure

Except for a small but consistent and statistically significant reduction of all the investigated dimensions (Fig. 8 and Table), chemical fixation does not modify the image of gap junctions as observed on freeze-fracture faces from quickly frozen heart tissues, and the slight decrease of the particles' distance is not sufficient to rearrange them in a more orderly appearance (Fig. 6). Both preparative procedures can therefore be considered to provide very similar pictures of heart gap junctions in whatever functional state.

By means of simpler but less rapid quick-freezing techniques employing liquid nitrogen or propane as coolants, Green and Severs (1984) have obtained freeze-fracture pictures of gap junctions which, in tissues frozen on the anesthetized animal, markedly differ from ours by the particle arrangement in multiple hexagonal arrays. Whatever the functional state of the junctions, P-face particles are never regularly ordered over large areas in our samples, and the connexons are as a rule randomly distributed as had been previously observed on gap junctions from quickly frozen mammalian heart (Baldwin, 1979) and epithelial tissues (Raviola et al., 1980).

Some Comments on the Uncoupling Effect of Glutaraldehyde

The quantitative data drawn in Figs. 7 and 8 show that glutaraldehyde does not systematically fix all gap junctions in a morphologically distinct uncoupled configuration, as might have been suspected from the large decrease in cell-to-cell conductance observed during the early action of this chemical on electrically coupled cell systems (Politoff & Pappas, 1972; Délèze & Hervé, 1983), since the change of the gap junctional dimensions with the functional state is still present in the junctions uncoupled prior to fixation by glutaraldehyde, on top of a systematic constricting effect of the fixative itself (Fig. 8), and since this change is quantitatively very similar to

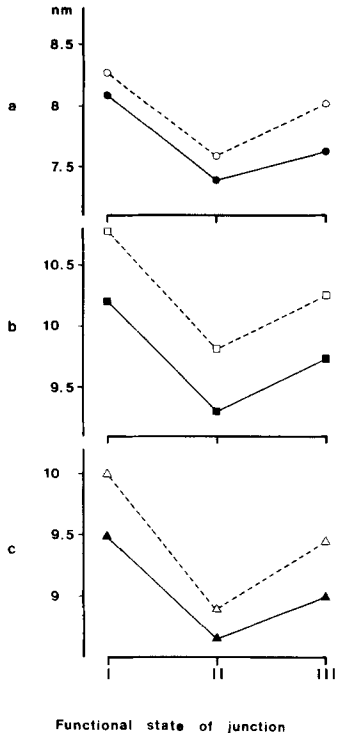

Fig. 8. Quantitative alterations of three gap junctional dimensions correlated with electrical uncoupling and recoupling, as observed on quickly frozen (open symbols and dotted lines) and glutaraldehyde-fixed (filled symbols and continuous lines) auricles. The functional states of the communicating junctions are indicated on the abscissa: (*I*) electrically coupled, (*II*) electrically uncoupled, (*III*) electrically recoupled. The mean dimensions reported on the ordinate are: (*a*) particle diameter, (*b*) particles' distance, (*c*) pits' distance. *See* Table for statistical parameters

that observed in the unfixed quickly frozen samples. This result indicates that glutaraldehyde promotes electrical uncoupling by a mechanism different from that induced by either DNP or heptanol. It is known that electrical uncoupling by DNP correlates with a rise of $[Ca^{2+}]_i$ (Rose & Loewenstein, 1976; Dahl & Isenberg, 1980). As a rise of $[Ca^{2+}]_i$ has also been observed in squid axons under the action of several aliphatic alcohols (Vassort et al., 1986), it seems possible to suggest that an increase of the cytosolic Ca^{2+} ion concentration triggers electrical uncoupling in DNP or heptanol-containing solutions, as it does in numerous other uncoupling experiments (Loewenstein, 1981).

On the other hand, the uncoupling effect of glutaraldehyde, a rapid and efficient protein cross-linker (Hopwood, 1972), might reflect a nonspecific plugging by polymerization of peptides or proteins inside the cell-to-cell channel or close to its mouth and have no bearing to a physiological cell-to-cell channel closure mechanism. The facts that electrical uncoupling during glutaraldehyde fixation is never complete (Délèze & Hervé, 1983) and has no

morphological correlate would agree with this argument.

A P-Face Particle Contraction Correlates with Electrical Uncoupling and is Partially Reversed after Recoupling

The morphological dimension which seems most directly related to the communicating function of the gap junction (the nexus, Dewey & Barr, 1962) is the reduction of the P-face particle's diameter, first observed by Peracchia and Dulhunty (1976) in the crayfish electrical synapse, since the pairs of opposite particles bridging the intercellular gap have been resolved into cylindrical hexameric protein structures enclosing a central hydrophilic channel (the connexon, Caspar et al., 1977; Makowski et al., 1977). It is therefore possible to suggest that their smaller diameter in the uncoupled cells might reflect the conformational transition that operates the shut-off mechanism of the channel. In a model developed by Unwin and Zampighi (1980) and Unwin and Ennis (1983, 1984), the structural change they observed on low angle X-ray diffraction images after Ca^{2+} addition to the preparation medium of isolated rat liver gap junctions is accounted for by a rotation and straightening up of the tilted connexon subunits with the largest tangential and radial displacements occurring at the cytoplasmic end, where the central hydrophilic channel could constrict by up to 18 Å (Unwin & Ennis, 1984). The decrease in connexon diameter of about 7 Å that we observe after controlled electrical uncoupling of living heart cells is certainly compatible with this model, since our measurements of the particle base close to the fracture plane, which lies in the central region of the membrane (McNutt & Weinstein, 1970), should approximately correspond to mid-distance from the hemi-connexon ends, wherein the model displacement would be half its maximum. This same argument would also account for the particle constriction of about 7 Å being smaller than the channel bore of 16 to 20 Å inferred from studies of the cell-to-cell permeabilities of different molecules (Schwarzmann et al., 1981).

A decrease in P-face particle diameter on uncoupling related to the operation of the channel shutoff mechanism is expected to be reversible when the cell-to-cell conductance is reestablished. We do show that morphological reversibility after recoupling is present though partial (about 50% of the difference between coupled and uncoupled gap junctions). It should be recalled here that it is not necessary that all cell-to-cell channels be in the opened state to detect a practically normal cell-to-cell electrical coupling (Délèze & Loewenstein, 1976; Socolar, 1977).

Although the changes in particle size measured after electrical uncoupling and recoupling are statistically significant, the values given should be considered as tentative estimates, because the replication technique by metal deposition on freeze-fractured tissues introduces distortions of the structure. Also, photographic enlargement somewhat blurs the transitions between lights and shadows, and measurement of particle diameters on prints contributes some further loss of accuracy. The last-mentioned sources of errors could be minimized in future work by a computer analysis of the densitometered negatives.

Is there a Correlation of Particle Distance and Functional State?

Although several investigators (Peracchia & Dulhunty, 1976; Peracchia, 1977; Baldwin, 1979; Raviola et al., 1980; Hanna et al., 1984; Miller & Goodenough, 1985) have looked for correlations between the distance and order of P-face particles and the functional state of the junctions, the functional significance of a tighter and more ordered connexon arrangement is by no means clear at present. We suggest that the primary conformational change occurring in the connexon when the cell-to-cell channel shuts off correlates with a measurable decrease of the junctional particle diameter. Other morphological changes, such as particle distance and arrangement, may be secondary to this initial event. Indeed, whatever intracellular signals control the channel patency, they are likely to act first on the active elements, the connexons, and not on the functionally more inert smooth membranes around them.

We wish to thank Dr. Michel Grosbras of the Physics Department for the loan of the particle size analyzer.

References

Abramowitz, M., Stegun, I.A. 1964. Handbook of Mathematical Functions, Applied Mathematics Series. Vol. 55. U.S. Department of Commerce, National Bureau of Standards

Baldwin, K.M. 1979. Cardiac gap junction configuration after an uncoupling treatment as a function of time. *J. Cell Biol.* **82**:66–75

Bernardini, G., Peracchia, C., Peracchia, L.L. 1982. Reversible gap junction crystallization and electrical uncoupling by heptanol. *Biophys. J.* **37**:285a

Bernardini, G., Peracchia, C., Peracchia, L.L. 1984. Reversible effects of heptanol on gap junction structure and cell-to-cell electrical coupling. *Eur. J. Cell Biol.* **34**:307–312

Brink, P., Barr, L. 1977. The resistance of the septum of the median giant axon of the earthworm. *J. Gen. Physiol.* **69**:517–536

Caspar, D.L.D., Goodenough, D.A., Makowski, L., Phillips, W.C. 1977. Gap junction structures. I. Correlated electron microscopy and X-ray diffraction. *J. Cell Biol.* **74**:605–628

Dahl, G., Isenberg, G. 1980. Decoupling of heart muscle cells: Correlation with increased cytoplasmic calcium activity and with changes of nexus ultrastructure. *J. Membrane Biol.* **53**:63–75

Délèze, J., Hervé, J.C. 1983. Effect of several uncouplers of cell-to-cell communication on gap junction morphology in mammalian heart. *J. Membrane Biol.* **74**:203–215

Délèze, J., Hervé, J.C. 1984. Effects of electrical uncoupling on the size and spacing of the gap junction particles in rat auricles examined after quick freezing at 6 °K. *J. Physiol. (London)* **351**:41P

Délèze, J., Loewenstein, W.R. 1976. Permeability of a cell junction during intracellular injection of divalent cations. *J. Membrane Biol.* **28**:71–86

De Mello, W.C. 1979. Effect of 2-4-dinitrophenol on intracellular communication in mammalian cardiac fibres. *Pfluegers Arch.* **380**:267–276

Dewey, M.M., Barr, L. 1962. Intercellular connections between smooth muscle cells: The nexus. *Science* **137**:670–672

Escaig, J. 1982. New instruments which facilitate rapid freezing at 83 K and 6 K. *J. Microsc. (Oxford)* **126**:221–229

Green, C.R., Severs, N.J. 1984. Gap junction connexon configuration in rapidly frozen myocardium and isolated intercalated disks. *J. Cell Biol.* **99**:453–463

Hanna, R.B., Pappas, G.D., Bennett, M.V.L. 1984. The fine structure of identified electrotonic synapses following increased coupling resistance. *Cell Tissue Res.* **235**:243–249

Harreveld, A. van, Crowell, J. 1964. Electron microscopy after rapid freezing on a metal surface and substitution fixation. *Anat. Rec.* **149**:381–386

Heuser, J.E., Reese, T.S., Landis, D.M.D. 1976. Preservation of synaptic structure by rapid freezing. *Cold Spring Harbor Symp. Quant. Biol.* **40**:17–24

Hopwood, D. 1972. Theoretical and practical aspects of glutaraldehyde fixation. *Histochem. J.* **4**:267–303

Johnston, M.F., Simon, S.A., Ramón, F. 1980. Interaction of anaesthetics with electrical synapses. *Nature (London)* **286**:498–500

Jongsma, H.J., Rijn, H.E. van 1972. Electrotonic spread of current in monolayer cultures of neonatal rat heart cells. *J. Membrane Biol.* **9**:341–360

Loewenstein, W.R. 1981. Junctional intercellular communication: The cell-to-cell membrane channel. *Physiol. Rev.* **61**:829–913

Makowski, L., Caspar, D.L.D., Phillips, W.C., Goodenough, D.A. 1977. Gap junction structures. II. Analysis of the X-ray diffraction data. *J. Cell Biol.* **74**:629–645

McNutt, N.S., Weinstein, R.S. 1970. The ultrastructure of the nexus. A correlated thin-section and freeze-cleave study. *J. Cell Biol.* **47**:666–688

Miller, T.M., Goodenough, D.A. 1985. Gap junction structures after experimental alteration of junctional channel conductance. *J. Cell Biol.* **101**:1741–1748

Noble, D. 1962. The voltage dependence of the cardiac membrane conductance. *Biophys. J.* **2**:381–393

Peracchia, C. 1977. Gap junctions: Structural changes after uncoupling procedures. *J. Cell Biol.* **72**:628–641

Peracchia, C., Dulhunty, A.F. 1976. Low resistance junctions in crayfish. Structural changes with functional uncoupling. *J. Cell Biol.* **70**:419–439

Politoff, A.L., Pappas, G.D. 1972. Mechanisms of increase in coupling resistance at electrotonic synapses of the crayfish septate axon. *Anat. Rec.* **172**:384–385

Politoff, A.L, Socolar, S.J., Loewenstein, W.R. 1969. Permeability of a cell membrane junction. Dependence on energy metabolism. *J. Gen. Physiol.* **53**:498–515

Raviola, E., Goodenough, D.A., Raviola, G. 1980. Structure of rapidly frozen gap junctions. *J. Cell Biol.* **87**:273–279

Rose, B., Loewenstein, W.R. 1976. Permeability of a cell junction and the local cytoplasmic free ionized calcium concentration: A study with aequorin. *J. Membrane Biol.* **28**:87–119

Schwabe, K.G., Terracio, L. 1980. Ultrastructural and thermocouple evaluation of rapid freezing techniques. *Cryobiology* **17**:571–584

Schwarzmann, G., Wiegandt, H., Rose, B., Zimmermann, A., Ben-Haim, D., Loewenstein, W.R. 1981. Diameter of the cell-to-cell junctional membrane channels as probed with neutral molecules. *Science* **213**:551–553

Shibata, Y., Page, E. 1981. Gap junctional structure in intact and cut sheep cardiac Purkinje fibers: A freeze-fracture study of Ca^{2+}-induced resealing. *J. Ultrastruct. Res.* **75**:195–204

Socolar, S.J. 1977. Appendix: The coupling coefficient as an index of junctional conductance. *J. Membrane Biol.* **34**:29–37

Socolar, S.J., Loewenstein, W.R. 1979. Methods for studying transmission through permeable cell-to-cell junctions. *In:* Methods in Membrane Biology. E. Korn, editor. Vol. 10, pp. 123–179. Plenum, New York

Tanaka, I., Sasaki, Y. 1966. On the electrotonic spread in cardiac muscle of the mouse. *J. Gen. Physiol.* **49**:1089–1110

Unwin, P.N.T., Ennis, P.D. 1983. Calcium-mediated changes in gap junction structure: Evidence from the low angle X-ray pattern. *J. Cell Biol.* **97**:1459–1466

Unwin, P.N.T., Ennis, P.D. 1984. Two configurations of a channel-forming membrane protein. *Nature (London)* **307**:609–613

Unwin, P.N.T., Zampighi, G. 1980. Structure of the junction between communicating cells. *Nature (London)* **283**:545–549

Vassort, G., Whittembury, J., Mullins, L.J. 1986. Increases in internal Ca^{2+} and decreases in internal H^+ are induced by general anesthetics in squid axons. *Biophys. J.* **50**:11–19

Weidmann, S. 1952. The electrical constants of Purkinje fibres. *J. Physiol. (London)* **118**:348–360

Woodbury, J.W., Crill, W.E. 1961. On the problem of impulse conduction in the atrium. *In:* Nervous Inhibition. E. Florey, editor. pp. 124–135. Pergamon, New York

Received 6 January 1986; revised 1 April 1986